CONSTRAINING THE ODD-HYDROGEN CHEMISTRY IN THE ATMOSPHERE OF MARS WITH THE EXOMARS TRACE GAS ORBITER

J. Alday, J. A. Holmes, M. R. Patel, J. P. Mason, *School of Physical Sciences, The Open University, Milton Keynes, UK (juan.alday@open.ac.uk),* **A. Trokhimovskiy, A. A. Fedorova, D. A. Belyaev, O. Korablev**, *Space Research Institute (IKI), Moscow, Russia,* **F. Lefèvre, F. Montmessin, L. Baggio, A. S. Braude,** *LATMOS, Guyancourt, France*, **K. S. Olsen, P. G. J. Irwin,** *AOPP, Department of Physics, University of Oxford, UK*, **C. F. Wilson,** *European Space Research and Technology Centre (ESTEC), Noordwijk, Netherlands.*

Introduction:

Odd-hydrogen (HO_x) species such as OH and HO_2 have a key role in regulating the chemistry of the atmosphere of Mars. This role was first evidenced by the slow recombination rate of the photolysis products of CO_2 (i.e., CO + O), which required a catalytic pathway to maintain a 95% CO_2 atmosphere on Mars. McElroy & Donahue (1972) and Parkinson & Hunten (1972) demonstrated that the stability of CO_2 in the Martian atmosphere holds due to reactions of its photolysis products with HO_x ($CO + OH \rightarrow CO_2 + H$), evidencing the importance of these photochemical species in the composition of the atmosphere.

The photochemistry of the martian atmosphere is frequently studied using remote sensing observations of O_3 (e.g., (Patel et al. (2021); Perrier et al. (2006)), CO (e.g., Olsen et al. (2021); Smith et al. (2021)) and H_2O_2 (e.g., Clancy et al. (2004); Encrenaz et al. (2008)), all of which are highly sensitive to the abundance of odd-hydrogen and often used as tracers of the HO_x chemistry.

Current numerical models of the atmosphere of Mars are able to explain the seasonal and latitudinal variations of these measured chemical tracers, generally showing good qualitative agreements between the measurements and the expectations (e.g., Holmes et al. (2018); Lefèvre (2004)). However, underestimation of the absolute abundances of O_3 and CO suggests that the model representation of HO_x oxidation is too efficient, which could be the result of some missing physical or chemical processes in the models, such as the uptake of HO_x on water ice clouds (Lefèvre et al., 2021; Lefèvre et al., 2008).

While the abundance of HO_x therefore seems crucial to understand the photochemical processes in the martian atmosphere, there is little information from measurements. Clancy et al. (2013) reported the first and only detection of OH on Mars, which consisted of infrared nightglow emissions in the polar winter atmosphere using from CRISM/MRO. On the other hand, HO_2 has never been detected in the martian atmosphere, with the most constraining upper limit (198 ppbv) being well above the expected abundances in 3D chemical models (Villanueva et al., 2013).

In this study, we search for infrared spectral signatures of OH and HO_2 in the atmosphere of Mars using solar occultation measurements by the Atmospheric Chemistry Suite (ACS) onboard the ExoMars Trace Gas Orbiter (TGO). In addition, we analyse the measurements in context with the expected abundances from the Mars Global Circulation Model (GCM) used by the modelling group at the Open University (hereafter OU-GCM).

ACS solar occultation observations:

ACS is one of the four instruments that comprise the payload of the ExoMars Trace Gas Orbiter. It consists of a suite of three spectrometers sampling different spectral ranges in the infrared: the near-infrared (NIR: 0.7-1.7 μm), the mid-infrared (MIR: 2.3-4.2 μm) and the thermal-infrared (TIRVIM: 0.7-17 μm) (Korablev et al., 2018).

In this work we use the MIR channel, which measures high-resolution spectra ($\lambda/\Delta\lambda \approx$ 20,000-30,000) and is dedicated to solar occultation observations. In this type of measurements, the Sun is continuously monitored from a tangent altitude of 270 km until it is occulted by the surface. The normalisation of the spectra using the reference solar signal measured at high altitudes (>120 km) allows us to generate a set of transmission spectra at different tangent heights. Solar occultations are especially suitable for the detection of trace gases in planetary atmospheres thanks to the use of the Sun as the light source, which results in high signal-to-noise ratio (SNR), and the long path sampled by the observations.

The dataset analysed in this work comprises all ACS MIR observations made using secondary grating position 3, which measures eight diffraction orders (206 to 213) encompassing a spectral range between 2.78-2.9 μm (3448-3597 cm^{-1}). Up to October 2021, there are 151 observations made using this specific position and covering a range between L_S = 160 in Martian Year 35 (MY35) and L_S = 60 in MY36.

Radiative transfer analysis:

The radiative transfer analysis of the observations

is performed using the NEMESIS algorithm (Irwin et al., 2008), which has previously been applied to the retrieval of isotopic ratios in the atmosphere from ACS solar occultations (e.g., Alday et al. (2021)). The spectral range sampled by ACS MIR secondary grating position 3 includes absorption features by CO_2, H_2O, OH and HO_2, whose absorption cross sections are computed with line-by-line modelling using the spectroscopic parameters from the 2020 edition of the HITRAN database (Gordon et al., 2022). In the case of the H_2O absorption, the pressure-broadening coefficients are updated based on the laboratory measurements of Devi et al. (2017) and Régalia et al. (2019), suitable for the broadening of the absorption lines in a CO_2-dominated atmosphere.

Figure 1 shows a forward model indicating the contribution of different gases to the spectra. The biggest challenge for the detection of HO_x in this spectral range is the removal of the absorption by CO_2, H_2O and dust to isolate the weak spectral features of OH and HO_2. While some of the strongest features of HO_x in the measured range are found for wavenumbers $\nu > 3500$ cm^{-1}, the absorption of CO_2 in that spectral range is much stronger than for $\nu < 3500$ cm^{-1}, which directly impacts the sensitivity of the measurements to these species. Therefore, we select five spectral windows in diffraction orders 206, 207 and 208 to perform our retrievals, as shown in Figure 1.

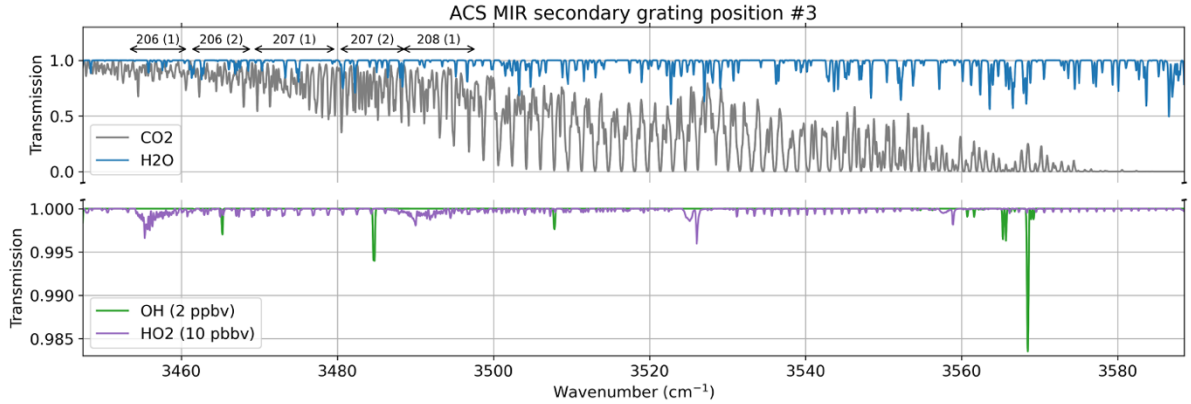

Figure 1: Forward model of a solar occultation observation made with ACS MIR secondary grating position 3 at a tangent altitude of 9 km, showing the contribution from different gases to the spectra, as indicated by the legend. The arrows represent the spectral range covered by each of the spectral windows in diffraction orders 206, 207 and 208 selected for the search of OH and HO_2.

The retrieval scheme is performed in two steps. First of all, vertical profiles of pressure and temperature are derived from the CO_2 absorption based on the hydrostatic equilibrium equation and a known volume mixing ratio, fitting these features together with the parameters describing the instrument line shape (Alday et al., 2019). Once the pressure and temperature profiles have been calculated, these are fixed, and a new set of retrievals is run to determine the volume mixing ratios of H_2O, OH and HO_2. The retrieved HO_x abundances are then evaluated based on the ratio between the retrieved abundance and uncertainty $\sigma = [HO_x]/[HO_x]_{err}$, where $\sigma > 3$ indicates a detection. On the other hand, when $\sigma < 3$, we define the 3σ upper limit using the retrieved uncertainties (UL = $3[HO_x]_{err}$).

Comparison with the OU-GCM:

Once the retrieved dataset for the HO_x species from the ACS observations is generated, the results will be compared with the expected abundances from the 3D chemical OU-GCM. This model shares physical parameterisations with the GCM from the Laboratoire de Mètèorologie Dynamique (LMD) (Forget et al., 1999), including the latest update of the photochemical module (Lefèvre et al., 2021).

In addition, the OU-GCM allows the assimilation of spacecraft data into the model. This combination of measurements and model constraints provides the best estimations for the HO_x abundance with the current physical and chemical parameterisations. The sets of assimilated data are similar to those in Holmes et al. (2022): temperature profiles and dust column from the Mars Climate Sounder on the Mars Reconnaissance Orbiter (MCS/MRO); water and ozone profiles, as well as water and carbon monoxide column abundances from the NOMAD instrument on the ExoMars TGO; temperature and water vapour profiles from ACS/TGO.

As these chemical species are tightly related to the HO_x chemistry, their assimilation provides useful constraints on the abundance of OH and HO_2 during the time period encompassed by the observations. These predicted model abundances will be compared with the results from the ACS dataset to evaluate if the observations can meaningfully constrain Mars' photochemical models. In addition, the expectations

from the model will also be used to maximise the sensitivity of the ACS measurements by averaging the spectra where the expected abundances in the model are highest.

Summary and conclusions:

Despite the key role odd-hydrogen species have in regulating the chemistry of the atmosphere of Mars, there is little direct information on the abundance of these from measurements. In this study, we aim to constrain the abundances of OH and HO_2 using solar occultation measurements from the ACS instrument on the ExoMars TGO. These measurements are ideal for the detection of trace species in the atmosphere of Mars thanks to the geometry of the observations.

We search for spectral signatures of these species using measurements made between 2.78-2.9 μm (3448-3597 cm^{-1}) between L_S = 160 in MY35 and L_S = 60 in MY36. These measurements allow the retrieval of pressure, temperature and water vapour volume mixing ratios during the whole period. In addition, the spectral signatures from OH and HO_2 allow the detection or derivation of upper limits at different altitudes, locations and time periods.

The results from these measurements will be compared with the expectations from the assimilation runs from the OU-GCM to test whether the measurements can meaningfully constrain Mars' photochemical models. In additions, these expectations from the model will also be used to establish a sensitive search at the times/locations when the abundance of HO_x is highest.

References:

Alday et al. (2019). Oxygen isotopic ratios in Martian water vapour observed by ACS MIR on board the ExoMars Trace Gas Orbiter. *A&A*, *630*, A91. doi/10.1051/0004-6361/201936234

Alday et al (2021). Isotopic fractionation of water and its photolytic products in the atmosphere of Mars. *Nature Astronomy*. doi/10.1038/s41550-021-01389-x

Clancy et al. (2004). A measurement of the 362 GHz absorption line of Mars atmospheric H2O2. *Icarus*, *168*(1), 116–121. doi/10.1016/j.icarus.2003.12.003

Clancy et al. (2013). First detection of Mars atmospheric hydroxyl: CRISM Near-IR measurement versus LMD GCM simulation of OH Meinel band emission in the Mars polar winter atmosphere. *Icarus*, *226*(1), 272–281. doi/10.1016/j.icarus.2013.05.035

Devi et al. (2017). Line parameters for CO_2- and self-broadening in the ν3 band of $HD^{16}O$. *JQSRT*, *203*, 158–174. doi/10.1016/j.jqsrt.2017.02.020

Encrenaz et al. (2008). Simultaneous mapping of H2O and H2O2 on Mars from infrared high-resolution imaging spectroscopy. *Icarus*, *195*(2), 547–556. doi/10.1016/j.icarus.2008.01.022

Forget et al. (1999). Improved general circulation models of the Martian atmosphere from the surface to above 80 km. *JGR: Planets*, *104*(E10), 24155–24175. doi/10.1029/1999JE001025

Gordon et al. (2022). The HITRAN2020 molecular spectroscopic database. *JQSRT*, *277*, 107949. doi/10.1016/j.jqsrt.2021.107949

Holmes et al. (2018). A reanalysis of ozone on Mars from assimilation of SPICAM observations. *Icarus*, *302*, 308–318. doi/10.1016/j.icarus.2017.11.026

Holmes et al. (2022). Global variations in water vapour and saturation state throughout the Mars Year 34 dusty season. *In review at JGP: Planets.*

Irwin et al. (2008). The NEMESIS planetary atmosphere radiative transfer and retrieval tool. *JQSRT*, *109*(6), 1136–1150. doi/10.1016/j.jqsrt.2007.11.006

Korablev et al. (2018). The Atmospheric Chemistry Suite (ACS) of Three Spectrometers for the ExoMars 2016 Trace Gas Orbiter. *Space Science Reviews*, *214*(1), 7. doi/10.1007/s11214-017-0437-6

Lefèvre (2004). Three-dimensional modeling of ozone on Mars. *JGR: Planets*, *109*(E7), E07004. doi/10.1029/2004JE002268

Lefèvre et al. (2021). Relationship Between the Ozone and Water Vapor Columns on Mars as Observed by SPICAM and Calculated by a Global Climate Model. *JGR: Planets*, *126*(4). doi/10.1029/2021JE006838

Lefèvre et al. (2008). Heterogeneous chemistry in the atmosphere of Mars. *Nature*, *454*(7207), 971–975. doi/10.1038/nature07116

McElroy & Donahue (1972). Stability of the Martian Atmosphere. *Science*, *177*(4053), 986–988. doi/10.1126/science.177.4053.986

Olsen et al. (2021). The vertical structure of CO in the Martian atmosphere from the ExoMars Trace Gas Orbiter. *Nature Geoscience*, *14*, 67–71. doi/10.1038/s41561-020-00678-w

Parkinson & Hunten (1972). Spectroscopy and Aeronomy of O_2 on Mars. *Journal of the Atmospheric Sciences*, *29*(7), 1380–1390. doi/10.1175/1520-0469(1972)029<1380:SAAOOO>2.0.CO;2

Patel et al. (2021). ExoMars TGO/NOMAD-UVIS Vertical Profiles of Ozone: 1. Seasonal Variation and Comparison to Water. *JGR: Planets, 126*(11), e2021JE006837.

Perrier et al. (2006). Global distribution of total ozone on Mars from SPICAM/MEX UV measurements. *JGR, 111*(E9), E09S06. doi.org/10.1029/2006JE002681

Régalia et al. (2019). Laboratory measurements and calculations of line shape parameters of the H2O–CO2 collision system. *JQSRT, 231*, 126–135. doi/10.1016/j.jqsrt.2019.04.012

Smith et al. (2021). The climatology of carbon monoxide on Mars as observed by NOMAD nadir-geometry observations. *Icarus, 362*, 114404. doi/10.1016/j.icarus.2021.114404

Villanueva et al. (2013). A sensitive search for organics (CH4, CH3OH, H2CO, C2H6, C2H2, C2H4), hydroperoxyl (HO2), nitrogen compounds (N2O, NH3, HCN) and chlorine species (HCl, CH3Cl) on Mars using ground-based high-resolution infrared spectroscopy. *Icarus, 223*(1), 11–27. doi/10.1016/j.icarus.2012.11.013